

# Investigation on gas-adsorption-induced swelling and permeability evolutions of CO<sub>x</sub> argillite

Haifeng YUAN<sup>a, b, \*</sup>, Franck AGOSTINI<sup>b</sup>, Frédéric SKOCZYLAS<sup>a, b</sup>,  
Jean TALANDIER<sup>c</sup>

- a. College of Civil and Architecture Engineering, Hubei University of Technology, Wuhan 430068, China.  
b. Laboratoire de Mécanique de Lille (LML), UMR 8107, and Ecole Centrale de Lille, BP 48, F-59651 Villeneuve d'Ascq Cedex, France  
c. Andra, 1-7 rue Jean Monnet, F-92298 Chatenay-Malabry Cedex, France

## Abstract :

*The main work of this contribution is to study the potential swelling capacity of CO<sub>x</sub> argillite induced by the gas adsorption. A series of gas injection tests was carried out by three kinds of gases with different adsorption capacities, i.e. helium (non-adsorbing gas), nitrogen (weakly adsorbing gas) and CO<sub>2</sub> (strong adsorbing gas). The results show the strain caused by CO<sub>2</sub> was larger than the strain caused by helium and nitrogen under the same gas pressure. This evidences the existence of the potential gas-adsorption-induced swelling pressure in argillite. In addition, the swelling strains exhibit an obvious anisotropic character, with larger deformation in direction perpendicular to bedding planes than those parallel to the bedding planes. This could be explained by the transverse isotropy structure of argillite. A series of gas permeability tests was also handed with the three gases. The results show that  $K(\text{CO}_2)$  is extremely low, about 10-19-10-20m<sup>2</sup>, compared with  $K(\text{helium})$  is about 10-18m<sup>2</sup> and  $K(\text{nitrogen})$  is about 10-19m<sup>2</sup>. This phenomenon could be further attributed to the swelling induced by gas adsorption which has narrowed the pore channel and caused the decrease of the gas permeability.*

**Key words :** CO<sub>x</sub> argillite; gas adsorption; swelling; gas permeability

## 1 Introduction

The swelling of coal and shale as the result of gas adsorption has been extensively studied in the context of some important projects, such as coalbed methane (CBM) production, carbon capture and storage (CCS), and shale gas production<sup>1-3</sup>. However, there are limited studies about the gas-adsorption-induced swelling of the argillaceous rocks, which have long been selected as the privileged candidate host rock for nuclear waste repository in many countries, such as Callovo-Oxfordian argillite (in France), Boom clay (in Belgium), and Opalinus clay (in Switzerland)<sup>4-6</sup>. In the long term sealing process, the possible leakage gases from the radioactive waste, which more or less has the adsorption capacity, will penetrate into the host rock and be adsorbed in clay minerals. Furthermore, considering the existence of swelling minerals in clayey rock, the gas adsorption changes surface potential energy of the adsorbent, leading to volumetric expansion followed by the adsorption-induced swelling pressure. The swelling pressure can not only potentially change the pore structure, but also change local stress regimes. These evolutions will possibly affect the gas transport property, micro- and macro- mechanical properties of the host rock. Therefore, in order to evaluate the sealing efficiency and safety of the geological repositories, it is important to study the gas-adsorption-induced swelling of the argillaceous rocks.

In this study, we focus on studying the potential swelling capacity of CO<sub>x</sub> argillite induced by the gas adsorption. In this context, a series of gas injection tests were handed by three different gases, helium, nitrogen, Carbon dioxide (CO<sub>2</sub>), respectively. The gas injection tests can study the adsorption capacity and corresponding swelling deformation of the three gases, further investigation about the longitudinal and transverse strain were also studied to show the swelling anisotropic properties. As helium is considered as non-adsorbing to clayey rock at ambient temperature, so we treat the tests with helium as a reference state in gas injection test. Lastly, gas permeability of these three gases was also conducted to verify the adsorption-induced swelling phenomenon.

## 2 Experimental methodology

### 2.1 Materials and sample preparation

The mineral compositions of the CO<sub>x</sub> argillite have long been studied by X-ray diffraction<sup>7, 8</sup>. It is general composed by clay matrix mixed with quartz and carbonate<sup>7</sup>. The content of the clay minerals is variable with the depth of the sample location, a high clay mineral content implies the argillite contains a high porosity, which provide more space for gas to reach and migrate. The dominate clay minerals are illite, kaolinite, chlorite and smectite, the smectite have a high gas adsorption swelling capacity, which may change the inner-structure and the effective stress of the host rock<sup>9, 10</sup>.

Two samples used in this study were cored from the T-cell, which were provided by Andra (*Agence nationale pour la gestion des déchets radioactifs*), with the reference EST51335-1 and EST51446-1. Small cylinder size, 20mm in diameter and 40mm in height, was used for the tests. These sample dimensions satisfy the standard requirement of the usual ratio (length/diameter=2), thus avoiding end effects and reducing the time needed to complete the gas injection tests. Before testing, the samples were dried at 60°C in the oven until a constant mass reached (no change for three consecutive days at ± 0.05%). After that, two cross-gauges were glued symmetrically on the surface of the sample EST51335-1 used to measure the strain evolution during the gas injection process.

### 2.2 Experimental setup

The adsorption-induced swelling and gas permeability tests were carried out using a self-designed apparatus in our laboratory (seen in Fig.1). The apparatus mainly consists by a hydrostatic cell, an oil pressure system, a gas injection system and a data acquisition system. The confining pressure of the system can reach up to 60MPa, and it is recorded by a manometer with the accuracy 0.01MPa. The gas injection pressure was supplied by three gas tank. Before the test, the volume of the reference cell was corrected by a standard reservoir. During the injection process, the gas injection pressure was continuously monitored by a pressure transducer with the accuracy 0.001MPa, and the pressure data was calibrated by the software Control Center Serie 30, which can record the pressure verse time and temperature verse time simultaneously. The apparatus was placed in a temperature-controlled room 20±2°C to ensure a constant temperature for the adsorption measurement.

### 2.3 Helium porosity measurements

Before all the measurement tests, a stainless steel sample with the same size of argillite sample was mounted in the cell to calibrate the volume of the tube, which was located between the reference cell and the sample. After that, the argillite sample was installed in the cell, and its porosity was firstly measured by helium. When the gas pressure was stable, we can consider that the gas in the argillite had reached equilibrium. Then based on the ideal gas law hypothesis, the accessible pore volume can be calculated by<sup>8</sup>:

$$V_{pore} = \frac{P_{ini}V_r}{P_{fi}} - (V_r + V_t) \quad (1)$$

Where  $P_{ini}$  and  $P_{fi}$  is the pressure before and after the equilibrium;  $V_r$  is the volume of the reference cell;  $V_t$  is the volume of the tube.

Then the porosity  $\phi_{He}$  is deduced from the volume of the sample  $V_{sample}$  as:

$$\phi_{He} = \frac{V_{pore}}{V_{sample}} \quad (2)$$

The helium porosity of argillite was measured under four pressure level: 10bar, 20bar, 30bar, 40bar. Attention should be paid that it is necessary to wait enough time to ensure the residual gas was dissipated from the sample in each gas pressure step. The confining pressure was maintained as 120bar in the measurement process, which is the same as the *in situ* hydrostatic pressure<sup>11</sup>.

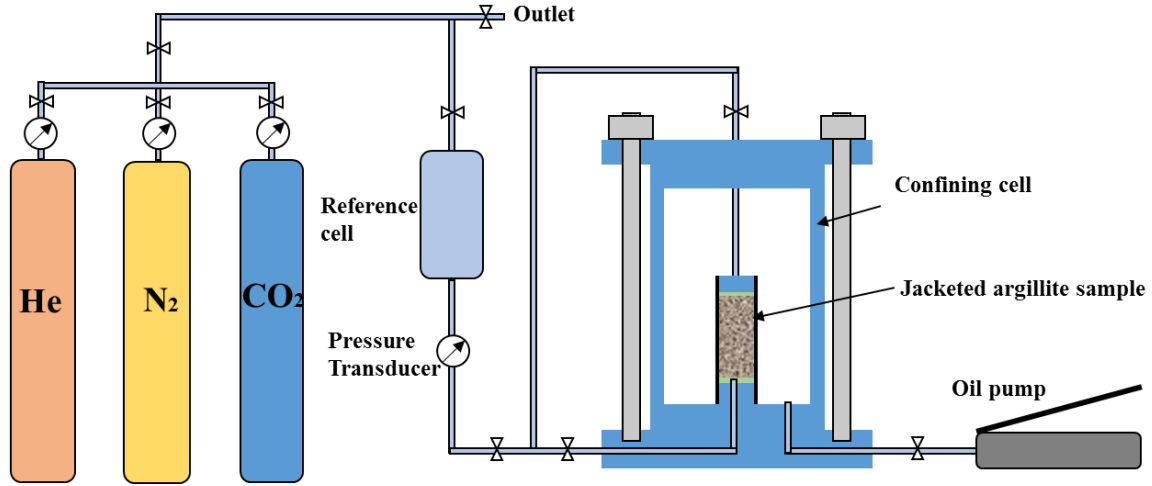


Fig.1. The schematic diagram of the experimental setup

## 2.4 Adsorption measurements

The adsorption measurements tests were handled by the same procedures as the helium porosity tests. The gas injection pressure and confining pressure were also the same as helium porosity tests in nitrogen and CO<sub>2</sub> adsorption tests. The main difference of the two tests is the calculation. During the adsorbing gas were injecting from the reference cell to the sample, the gas pressure would decrease due to the void volume filling as well as adsorption. Therefore, for each gas injection step, the amount of Gibbs adsorption (also called excess adsorption) can be calculated by the equation<sup>12</sup>:

$$n_m = \frac{P_{ini}V_r}{RT} - \frac{P_{pore}(V_r+V_t+V_p)}{RT} \quad (3)$$

Where  $n_m$  is the Gibbs adsorption amount in moles;  $P_{ini}$  is the initial injection pressure;  $P_{pore}$  is the final pressure after equilibrium;  $V_p$  is the volume of the pores occupied by helium;  $R$  is the universal gas constant; and  $T$  is the temperature.

Gibbs adsorption amount neglects the volume occupied by the adsorbed phase in calculating the amount of adsorbed gas. Based on the Gibbs adsorption amount, the absolute adsorption was estimated using the equation<sup>10, 13, 14</sup>:

$$n_{abs} = \frac{n_m}{1 - \frac{p}{\rho_{abs}}} \quad (4)$$

Where  $n_{abs}$  is the absolute adsorption amount and  $\rho_{abs}$  is the density of the adsorbed phase. In this contribution, we used the absolute adsorption amount to evaluate the potential adsorption capacity of N<sub>2</sub> and CO<sub>2</sub> in argillite.

## 2.5 Swelling measurements

During each gas injection step, no matter helium, nitrogen or CO<sub>2</sub>, the transverse and longitudinal strains were recorded by the strain gauges simultaneously. We regard the deformation caused by helium gas injection as a reference state to calculate the swelling deformation of nitrogen and CO<sub>2</sub>. Then the swelling deformation can be calculated by:

$$\varepsilon_{swelling} = \varepsilon_{N_2 \text{ or } CO_2} - \varepsilon_{helium} \quad (5)$$

## 2.6 Gas permeability measurements

After each gas injection step, the valve in the upside of the cell is demounted and instead by a gas pressure capture to measure the gas permeability of the three gases in each gas pressure level. The gas permeability is calculated by Darcy's law:

$$K = \frac{\mu_g Q_{mean}}{A} \frac{2hP_{mean}}{(P_{mean}^2 - P_0^2)} \quad (6)$$

Where h is the height of sample, A is the sample cross-sectional area,  $\mu_g$  is gas viscosity.  $Q_{mean}$  is the average flowrate in a short time  $\Delta t$ , and it is get by<sup>15</sup>:

$$Q_{mean} = - \frac{V_r \Delta P_1}{P_{mean} \Delta t} \quad (7)$$

where  $P_{mean} = P_0 - \Delta P_1 / 2$ ,  $\Delta P_1$  is the gas pressure drop in  $\Delta t$ .

## 3 Results

### 3.1 Helium porosity

The results of helium porosity are shown in Fig.2. It can be seen that the measured porosity of argillite slightly increases as the gas pressure increase from 10bar to 40bar, at constant hydrostatic pressure of 120bar. The helium porosity increases from 12.882% to 13.123% for sample EST51446-1, and from 11.454% to 11.708% for sample EST51335-1. These slightly increases also indicate that the gas can access to most of the accessible pores when gas pressure is 10bar.

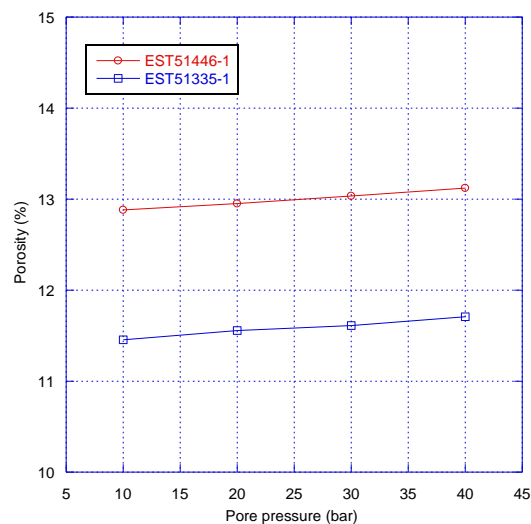


Fig.2. Helium porosity with respect to gas pressure at  $P_c=120$ bar

### 3.2 Adsorption

Experimental data for nitrogen and CO<sub>2</sub> absolute adsorption isotherms of sample EST51446-1 and EST51335-1 were collected by the volumetric method. The Gibbs adsorption and absolute adsorption masses can be calculated according to eqs. (3) and (4). The absolute density of nitrogen and CO<sub>2</sub> was assumed to be 0.808g/ml and 1.18g/ml in the ambient temperature. The results of the absolute adsorption isotherms of the two samples are shown in Fig.3. It is clear that both of the two gases are adsorbable in argillite, and CO<sub>2</sub> have an obvious stronger adsorption capacity than nitrogen. For example, the absolute adsorption amount of CO<sub>2</sub> in sample EST51446-1 is 0.124mmol/g when pore pressure is 40bar, while this value of is 0.029 mmol/g when tested by nitrogen in the same pore pressure. The same phenomenon have been observed in coal and shale<sup>16, 17</sup>. We can also observe that the adsorption isotherms for both two samples follow the trend of a typical Langmuir-type adsorption isotherm<sup>12, 18</sup>. Further experiment need to be conducted to study the Langmuir parameters of this typical clayey rock suffered to the adsorbable gas penetration. In addition, in order to make a clear understanding of the gas adsorption of argillite, the results of total gas and absolute isotherms of sample EST51446-1 were plotted in Fig.4. It

is shown that the total gas amount is nearly increase linearly with the gas pressure, while the absolute isotherms show as a Langmuir-type adsorption isotherm. This is owing to that, as adsorption occurs in the meso- and micro- pores, the pores occupied by the adsorbed gas that is no longer accessible to free gas<sup>10</sup>. In other words, the adsorption capacity is going to be saturated with the increase of the gas pressure.

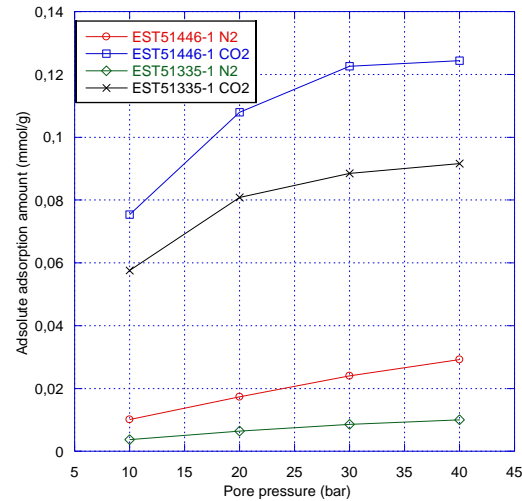


Fig.3. Nitrogen and CO<sub>2</sub> absolute adsorption isotherms results of two argillite samples

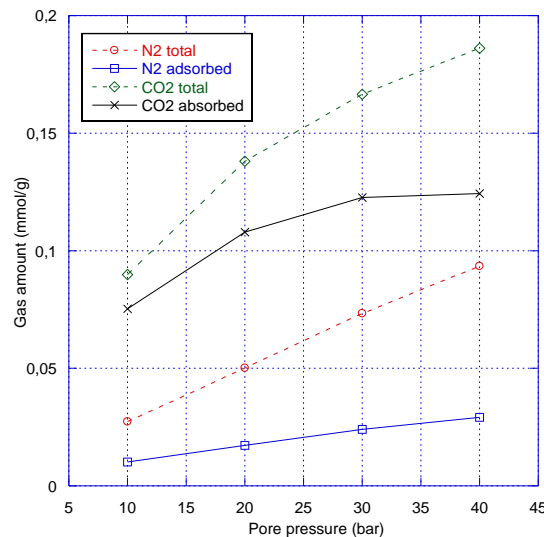


Fig.4. Nitrogen and CO<sub>2</sub> total gas and absolute adsorption isotherms of sample EST51446-1

### 3.3 Swelling

Fig.5 shows the evolution of volumetric strain of sample EST51335-1 caused by injecting helium, nitrogen and CO<sub>2</sub>, respectively. Here, we regard the swelling strain as a positive value, which is widely accepted in the literatures for gas-induced swelling. As shown in Fig.5, the volumetric strain is increased with the increase of gas pressure, this is due to the effective stress is decreased with the increase of gas pressure, which causes the increase of swelling strain. It is also clear that the volumetric strain caused by injecting CO<sub>2</sub> is far larger than the volumetric strain caused by injecting nitrogen and helium, and the volumetric strain caused by nitrogen is slightly larger than helium. These different swelling deformation, indicate that the swelling strain is not only caused by the poroelasticity effects, but also caused by some unknown effects. Combine with the former results about nitrogen and CO<sub>2</sub> adsorption in argillite, it is reasonable to suspect that the gas adsorption can induce an extra swelling strain of argillite. In fact, this adsorption-swelling deformation have widely observed in clayey rocks<sup>19, 20</sup>.

Fig.6 shows the longitudinal and transverse adsorption-induced swelling strain of sample EST51335-1 caused by injecting nitrogen and CO<sub>2</sub>. It is obvious to observe that the adsorption-induced swelling strain shows the anisotropic characters. For the two gases adsorption processes, the longitudinal strains are greater than the transverse strains. As shown in Fig.6, the longitudinal strain caused by CO<sub>2</sub> adsorption increases nearly 9 times when gas pressure increases from 10bar to 40bar, while the transverse strain increases nearly 8 times in the same gas pressure increment. These anisotropic swelling characters are the same as the strain results on shales<sup>10, 21</sup>, and possibly owing to the anisotropy pore structure as well as the mechanics properties<sup>22</sup>. In addition, Fig.6 also shows that the also the CO<sub>2</sub> adsorption-induced swelling deformation is larger than the nitrogen adsorption-induced swelling strain in both directions, due to the different adsorption-swelling capacities of these two gases.

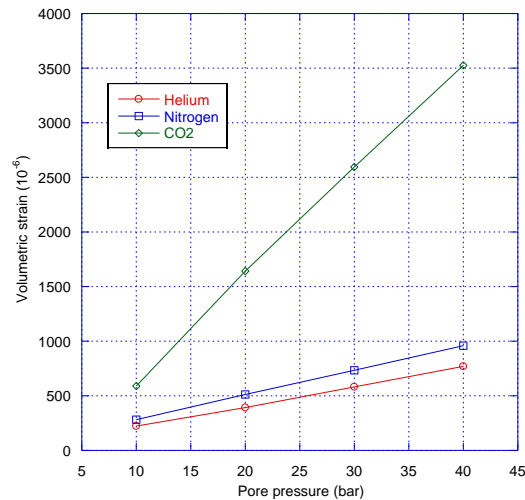


Fig.5. The volumetric strain of sample EST51335-1 as a function of injection gas pressure

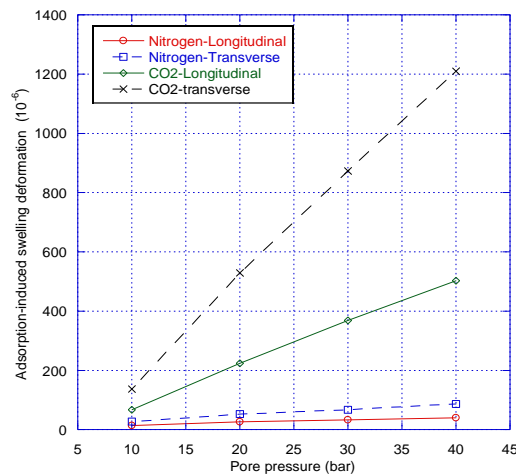


Fig.6. The adsorption-induced swelling strain of sample EST51335-1 as a function of injection gas pressure

### 3.4 Gas permeability

Fig.7 presents the gas permeability of the two samples measured by helium, nitrogen and CO<sub>2</sub>, respectively. It can be observed that  $K(\text{helium})$  is relatively high (around  $10^{-18}\text{-m}^2$ ),  $K(\text{nitrogen})$  is an immediate state (around  $10^{-19}\text{m}^2$ ), while  $K(\text{CO}_2)$  is extremely low (around  $10^{-19}\text{-}10^{-20}\text{m}^2$ ). It can be explained by the gas adsorption effect to the gas permeability of argillite. When the gas is absorbed in the meso- and micro- pores, it will induce the macroporosity change, which in turn results in the change of permeability<sup>23</sup>. Moreover, the different order of the permeability measured by three gases is owing to the different gas adsorption capacities of them.

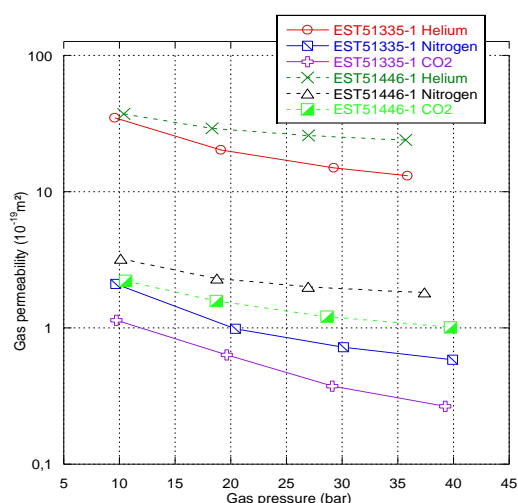


Fig.7. Gas permeability results of two argillite samples

## 4 Conclusion

Our experimental investigation evidence the gas-adsorption-induced swelling of argillite. Considered the helium injection tests as a reference state, the adsorption of nitrogen and CO<sub>2</sub> were investigated. The results show that, unlike non-adsorbing of helium, the nitrogen is weakly adsorbed, while the CO<sub>2</sub> is strongly adsorbed in argillite. The tested results are very similar to the results got by shale<sup>10, 32</sup>, as all of them contains clay minerals, which have abundant micropores. The adsorbable gas can easily adsorbed in the micropores. Furthermore, the obvious adsorption-swelling deformations were observed when using nitrogen and CO<sub>2</sub> as the injection gas. These are owing to the swelling minerals, such as smectite and I/S (illite/smectite), in claymatrix. Therefore, when adsorbable gas is penetrates in argillite, it is not a purely poroelasticity problems, the swelling pressure will also affect to the effective stress. The adsorption-swelling deformation shows an anisotropic character, this could be explained by the transverse isotropy structure of argillite. Lastly, the permeability tests carried out by helium, nitrogen and CO<sub>2</sub> illustrate that the adsorption also has a significant effect to the gas permeability. This is owing to the gas-adsorption-swelling deformation, which can narrow the gas transport channels in argillite.

## Acknowledgments

The authors greatly acknowledged Andra for its material and financial supports provided in this work.

## References

- [1] Zang J, Wang K. Gas sorption-induced coal swelling kinetics and its effects on coal permeability evolution: Model development and analysis. *Fuel*. 2017;189: 164-177.
- [2] Zang J, Wang K, Zhao Y. Evaluation of gas sorption-induced internal swelling in coal. *Fuel*. 2015;143: 165-172.
- [3] Mazumder S, Karnik AA, Wolf K-HAA. Swelling of Coal in Response to CO<sub>2</sub> Sequestration for ECBM and Its Effect on Fracture Permeability.
- [4] Yuan H, Agostini F, Duan Z, Skoczylas F, Talandier J. Measurement of Biot's coefficient for CO<sub>x</sub> argillite using gas pressure technique. *Int J Rock Mech Min Sci*. 2017;92: 72-80.
- [5] Jacobs E, Volckaert G, Maes N, Weetjens E, Govaerts J. Determination of gas diffusion coefficients in saturated porous media: He and CH<sub>4</sub> diffusion in Boom Clay. *Appl Clay Sci*. 2013;83-84: 217-223.
- [6] Favero V, Ferrari A, Laloui L. On the hydro-mechanical behaviour of remoulded and natural Opalinus Clay shale. *Eng Geol*. 2016;208: 128-135.
- [7] Zhang F, Xie SY, Hu DW, Shao JF, Gatmiri B. Effect of water content and structural anisotropy on

- mechanical property of claystone. *Appl Clay Sci.* 2012;69(0): 79-86.
- [8] Song Y, Davy CA, Bertier P, Skoczylas F, Talandier J. On the porosity of CO<sub>x</sub> claystone by gas injection. *Microporous and Mesoporous Materials.* 2017;239: 272-286.
- [9] Guo S. Experimental study on isothermal adsorption of methane gas on three shale samples from Upper Paleozoic strata of the Ordos Basin. *J Pet Sci Technol.* 2013;110: 132-138.
- [10] Heller R, Zoback M. Adsorption of methane and carbon dioxide on gas shale and pure mineral samples. *Journal of Unconventional Oil and Gas Resources.* 2014;8: 14-24.
- [11] Andra. Dossier 2005 Argile. Collection Les Rapports. 2005.
- [12] Wang Y, Liu S. Estimation of Pressure-Dependent Diffusive Permeability of Coal Using Methane Diffusion Coefficient: Laboratory Measurements and Modeling. *Energy & Fuels.* 2016.
- [13] Liu S, Harpalani S. A new theoretical approach to model sorption-induced coal shrinkage or swelling. *AAPG Bulletin.* 2013;97(7): 1033.
- [14] Liu S, Wang Y, Harpalani S. Anisotropy characteristics of coal shrinkage/swelling and its impact on coal permeability evolution with CO<sub>2</sub> injection. *Greenhouse Gases: Science and Technology.* 2016;6(5): 615-632.
- [15] Liu J-F, Song Y, Skoczylas F, Liu J. Gas migration through water-saturated bentonite–sand mixtures, CO<sub>x</sub> argillite, and their interfaces. *Canadian Geotechnical Journal.* 2015;53(1): 60-71.
- [16] Fitzgerald JE, Pan Z, Sudibandriyo M, Robinson JRL, Gasem KAM, Reeves S. Adsorption of methane, nitrogen, carbon dioxide and their mixtures on wet Tiffany coal. *Fuel.* 2005;84(18): 2351-2363.
- [17] Li X, Feng Z, Han G, et al. Breakdown pressure and fracture surface morphology of hydraulic fracturing in shale with H<sub>2</sub>O, CO<sub>2</sub> and N<sub>2</sub>. *Geomechanics and Geophysics for Geo-Energy and Geo-Resources.* 2016;2(2): 63-76.
- [18] Singh H, Javadpour F. Langmuir slip-Langmuir sorption permeability model of shale. *Fuel.* 2016;164: 28-37.
- [19] Busch A, Bertier P, Gensterblum Y, et al. On sorption and swelling of CO<sub>2</sub> in clays. *Geomechanics and Geophysics for Geo-Energy and Geo-Resources.* 2016;2(2): 111-130.
- [20] Mosher K, He J, Liu Y, Rupp E, Wilcox J. Molecular simulation of methane adsorption in micro- and mesoporous carbons with applications to coal and gas shale systems. *International Journal of Coal Geology.* 2013;109–110: 36-44.
- [21] Lu Y, Ao X, Tang J, Jia Y, Zhang X, Chen Y. Swelling of shale in supercritical carbon dioxide. *Journal of Natural Gas Science and Engineering.* 2016;30: 268-275.
- [22] Pan Z, Connell LD. Modelling of anisotropic coal swelling and its impact on permeability behaviour for primary and enhanced coalbed methane recovery. *International Journal of Coal Geology.* 2011;85(3–4): 257-267.
- [23] Li CJ, Feng JL. Adsorption-induced permeability change of porous material: a micromechanical model and its applications. *Archive of Applied Mechanics.* 2016;86(3): 465-481.
- [24] Kazemi M, Takbiri-Borujeni A. An analytical model for shale gas permeability. *International Journal of Coal Geology.* 2015;146: 188-197.